

Experimental Evidence of ${}^2\text{He}$ Decay from ${}^{18}\text{Ne}$ Excited States

G. Raciti,* G. Cardella, M. De Napoli, E. Rapisarda, F. Amorini, and C. Sfienti

Dipartimento di Fisica e Astronomia, Università di Catania Via S. Sofia 64, I-95123, Catania, Italy

INFN—Sezione di Catania, Via S. Sofia 64, I-95123, Catania, Italy

(Received 21 December 2007; published 15 May 2008)

Two-proton decay from ${}^{18}\text{Ne}$ excited states has been studied by complete kinematical reconstruction of the decay products. The ${}^{18}\text{Ne}$ nucleus has been produced as a radioactive beam by ${}^{20}\text{Ne}$ primary projectile fragmentation at 45 AMeV incident energy on a Be target. The ${}^{18}\text{Ne}$ at 33 AMeV incident energy has been excited via Coulomb excitation on a ${}^{\text{nat}}\text{Pb}$ target. The obtained results unambiguously show that the 6.15 MeV ${}^{18}\text{Ne}$ state two-proton decay proceeds through a ${}^2\text{He}$ diproton resonance (31%) and democratic or virtual sequential decay (69%). The quoted branching ratio has been deduced from relative angle and momentum correlations of the emitted proton pairs.

DOI: [10.1103/PhysRevLett.100.192503](https://doi.org/10.1103/PhysRevLett.100.192503)

PACS numbers: 23.50.+z, 25.60.-t, 25.70.De, 27.20.+n

The simultaneous emission of two protons ($2p$) was proposed more than 40 years ago as a possible decay mode for even- Z -nuclei beyond or close to the proton drip line [1]. However, this decay mode is, in general, in competition with the sequential decay, where the two protons are sequentially emitted via an intermediate state of the $Z - 1$ daughter nucleus. In those cases where the sequential decay is energetically forbidden, a simultaneous $2p$ -emission should remain the only possible decay mode [2]. Over the last decades, many experimental studies [3] produced results consistent with a sequential decay description. The first observations of $2p$ simultaneous radioactivity has been reported for the ${}^{17}\text{Ne}$ [4,5], ${}^{45}\text{Fe}$ [6,7], ${}^{54}\text{Zn}$ [8], ${}^{48}\text{Ni}$ [9], ${}^{18}\text{Ne}$ [10], and more recently for ${}^{94}\text{Ag}$ [11] and ${}^{19}\text{Mg}$ [12]. However, two different decay modes for simultaneous $2p$ emission are possible: (i) three-body direct breakup involving an uncorrelated emission of the two protons, usually referred to as democratic emission [13], (ii) ${}^2\text{He}$ cluster emission where a pair of protons, correlated in a quasibound 1S configuration, breakup, when emitted, into two protons (diproton emission) [2]. It has been proposed to experimentally distinguish these two decay modes by studying proton-proton angle- and energy-correlations [2]. Among others [3], such a study was applied to the $2p$ decay of the 6.15 MeV (1^-) level of ${}^{18}\text{Ne}$, populated through the fusion reaction ${}^{17}\text{F} + p$ [10]. This decay was considered very promising since the 6.15 MeV (1^-) level is located in an energy window where sequential decay through ${}^{17}\text{F}$ is energetically forbidden (see Fig. 1, top panel). Unfortunately, the relative proton-proton energy and angle spectra analysis did not allow to distinguish between diproton and democratic emission. Moreover, by the evaluation of the resonant two-proton production cross section and $1p$ and $2p$ branching ratios by means of the R -matrix theory, in Ref. [14], it was concluded that the observed $2p$ events are unlikely attributed to the 6.15 MeV level decay, and probably they are produced by the ${}^{17}\text{F}$ projectile breakup. On the other hand, by the generalization of the Shell Model Embedded in the Continuum (SMEC) formalism [15] to include two parti-

cles in the scattering continuum [16], it has been pointed out that the $2p$ decay of the 6.15 MeV state reported in Ref. [10] can be explained as a sequential process through the correlated scattering continuum of ${}^{17}\text{F}$ (virtual sequential decay) and, possibly, a weak diproton branch. However, very little is known both from the experimental and theoretical point of view on the ${}^{18}\text{Ne}$ nucleus. The only known levels are reported in Fig. 1 (top panel). Therefore, with the aim to investigate both ${}^{18}\text{Ne}$ nuclear levels and their diproton decay, we performed an experiment by using the ${}^{18}\text{Ne}$ radioactive beam produced at the in-Flight Radioactive Ion Beams (FRIBs) facility [17] of the Laboratori Nazionali del Sud (LNS)-Italy.

The secondary ${}^{18}\text{Ne}$ beam has been selected among the fragmentation products of a primary stable ${}^{20}\text{Ne}$ beam at 45 AMeV, delivered by the LNS Superconductor Cyclotron (SC), on a ${}^9\text{Be}$, 500 μm thick, production target. The secondary ions have been separated in-flight in the fragment separator of the LNS operating at a $B\rho$ setting optimized for the ${}^{18}\text{Ne}$ transmission, with a momentum acceptance of $\pm 1.25\%$. A primary current of 300 enA produced a total RIBs rate of 10^5 ions/sec at the exit of the fragment separator. The secondary beam has been transported with 60% transmission up to the scattering chamber. Therefore, since the ${}^{18}\text{Ne}$ was about 9% of the total RIBs mixture, we had a rate of about 5.5×10^3 pps on the secondary target. Each ion of the incoming beam cocktail was tagged, on an event-by-event basis, in terms of Z , A , and energy by a 16×16 Double-Sided Si-Strip detector (DSSD) 300 μm thick and 5×5 cm^2 of active area (tagging detector) [17] before the interaction on the secondary 215 μm thick ${}^{\text{nat}}\text{Pb}$ target. The ion identification was performed by the ΔE -ToF technique (Fig. 1, bottom panel). The energy loss ΔE was measured by the Si-Strip detector. From the same signal, the stop pulse to measure the time-of-flight (ToF) of the ion, with respect to the radio frequency signal provided by the SC, was derived.

Fragments and particles produced in the interaction with the secondary target were identified in Z , A , energy, and

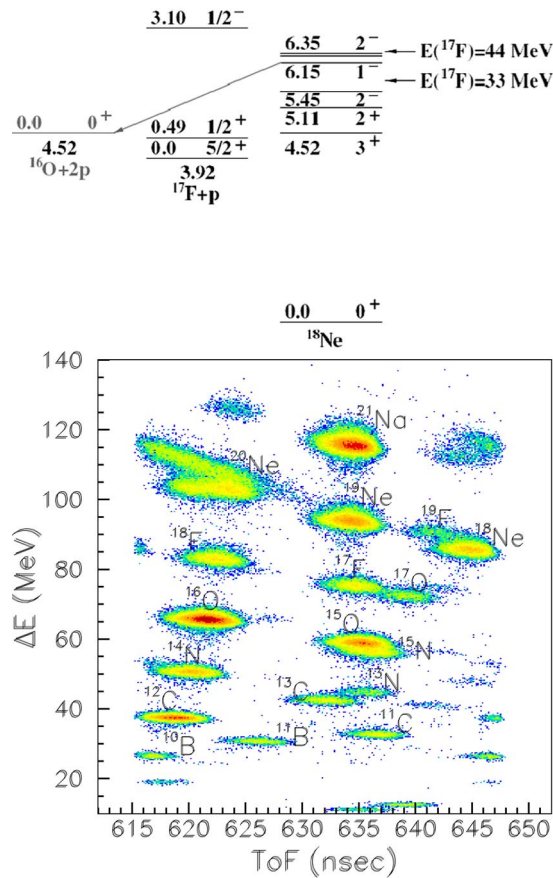


FIG. 1 (color online). Top panel: Level scheme of ^{18}Ne from Ref. [10]. Bottom panel: Energy loss in the DSSD versus ToF.

angle by a detection setup consisting of two Si-CsI hodoscopes. The first is composed of 81 twofold 1×1 cm² of active area telescopes: 300 μm Si detectors followed by a 10 cm long CsI(Tl). It covers, in steps of $\pm 0.6^\circ$ both in θ and ϕ , the spherical surface around zero degree with an opening angle of $\theta = \pm 5^\circ$. The second hodoscope consists of 89 threefold 3×3 cm² surface telescopes: 50 μm + 300 μm Si detectors followed by a 6 cm long CsI(Tl). It covers, in steps of $\pm 1.5^\circ$ in θ and ϕ , the spherical surface of the solid angle between $\pm 5^\circ$ and $\pm 21.5^\circ$. CsI scintillators were read out by photodiodes. The whole array covers 0.34 sr of the forward solid angle, including zero degree, with a geometrical efficiency of 72%. According to Monte Carlo simulations, its granularity and low thresholds allow to detect coincident ^{16}O - p - p events with 30% efficiency.

The ^{18}Ne projectile has been selected by gating on the ΔE -ToF plot provided by the tagging detector (Fig. 1, bottom panel). The X - Y coordinates of the interaction point on the DSSD as well as the incident energy on the $^{\text{nat}}\text{Pb}$ target were also measured on an event-by-event basis. The ^{18}Ne incident energy was in the range of 33 ± 1.2 AMeV (FWHM) as evaluated from the measured energy loss in the Si-Strip and measured in the telescopes around and at zero degree in empty target runs. Those runs were also

used to subtract the background produced by reactions on the DSSD from the data. The spread in the projectile energy of $\pm 3.7\%$ was due both to the $\Delta E/E$ acceptance of the fragment separator ($\pm 2.5\%$) and to the straggling in the tagging detector ($\pm 1.2\%$). The latter produced a beam angular straggling of 0.5° FWHM. From the velocities and angles of the decay products measured in coincidence in the hodoscopes, the center of mass (CM) velocity was reconstructed. This procedure was first applied to the $^{12}\text{C} + \alpha$ decay channel of the ^{16}O beam, selected by gating on the ΔE -ToF plot of Fig. 1 (bottom panel). The ^{16}O reconstructed incident velocity distribution was in good agreement with the one simulated by the LISE code [18] where both the angular and energetic straggling in the thick $^{\text{nat}}\text{Pb}$ target and in the DSSD were added to the $\Delta p/p$ acceptance of the fragment separator. Through an iterative procedure based on energy conservation, the position of interaction within the target was determined within a resolution of ± 50 μm [19]. The procedure allowed to distinguish between events coming from the Pb target and those coming from the tagging detector (background). Moreover, in order to select very peripheral reactions, only events in which the residue was detected at small emission angles, and both particles and residue had velocities close to that of the incident beam were chosen. The excitation energy spectrum of ^{16}O shown in Fig. 2 (left panel) was obtained by using the Q value for the $^{12}\text{C} + \alpha$ decay channel and the reconstructed incident beam energy values. Though the energy resolution was only 500 keV, the spectrum mainly exhibits the well-known 1^- and 2^+ ^{16}O levels as expected for the Coulomb excitation process. With the same procedure, the excitation-energy spectra of ^{18}Ne were reconstructed from the $^{17}\text{F} + p$ and $^{16}\text{O} + 2p$ events (Fig. 2, right panel). The low-lying ^{18}Ne 5.09 MeV (2^+) and 5.15 MeV (2^+) energy levels [20], although partially superimposed, can be recognized only in the $^{17}\text{F} + p$ decay channel because of the lower mass-excess value (3.92 MeV) with respect to the $^{16}\text{O} + 2p$ channel (4.52 MeV). The presence of the 6.15 MeV (1^-) peak both in the $^{17}\text{F} + p$ and $^{16}\text{O} + 2p$ channels confirms the observation of one- and two-proton decay of this ^{18}Ne state reported in Ref. [10]. From this level, the sequential $2p$ decay channel through a ^{17}F level is energetically forbidden (Fig. 1, top panel). The $2p$ decay from the known 7.06 MeV (1^- or 2^+), 7.91 MeV (1^- or 2^+), and 8.5 MeV levels is also observed, but, for these levels, the sequential $2p$ decay channel is available. The populated known ^{18}Ne levels are essentially 1^- and 2^+ states suggesting again the Coulomb excitation as the main reaction channel. Therefore, we propose 1^- or 2^+ spin assignment for the unknown high-lying states at around 8.5 MeV, 10.7 MeV, 12.5 MeV, and 13.7 MeV. Moreover, since they are not observed in the $^{17}\text{F} + p$ decay channel, their branching ratio to the $1p$ channel should be negligible.

In order to investigate whether the observed $2p$ -decay of the 6.15 MeV level proceeds through diproton, democratic or virtual sequential, the relative angle and momentum

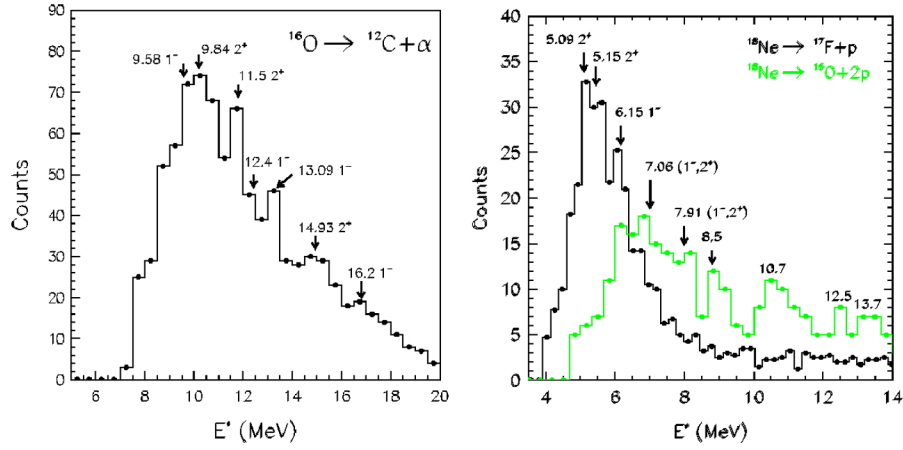


FIG. 2 (color online). Left panel: Excitation-energy spectrum of ^{16}O from $^{12}\text{C} + \alpha$ events. Right panel: Excitation-energy spectrum of ^{18}Ne from $^{16}\text{O} + 2p$ events and from $^{17}\text{F} + p$ channel (scaled 1/4). The levels values are from Ref [20].

spectra of the two emitted protons in the $^{16}\text{O} + 2p$ CM system (Fig. 3) have been analyzed. Events were selected in the excitation-energy window $5.9 \leq E^* \leq 6.5$ MeV, and the spectra were compared with Monte Carlo simulations.

Ingredients of the simulation code were the decay mechanism (sequential or simultaneous two-proton decay), the excitation-energy width taken from Ref. [20], the measured beam properties (angular divergence, incident energy) and the detection setup efficiency. The ^2He decay (dotted curve in Fig. 3), was evaluated by randomly sampling the phase-space of the two-step process $^{18}\text{Ne} \rightarrow ^{16}\text{O} + ^2\text{He} \rightarrow ^{16}\text{O} + p + p$ with the constraints of energy and momentum conservation [21]. The democratic decay (dashed curve in Fig. 3) was simulated in the same way but sampling the phase-space of the three-body ($^{16}\text{O} + p + p$) final state. Both the simulations of the virtual sequential decay through the correlated scattering continuum states ($5/2^+$ and $1/2^+$) of ^{17}F [16] (dot-dashed curve in Fig. 3) and the true sequential decay through the 3.10 MeV ($1/2^-$) ^{17}F level, when allowed, were evaluated by sampling the two-step process $^{18}\text{Ne} \rightarrow ^{17}\text{F} + p \rightarrow ^{16}\text{O} + p + p$ with the same constraints. The simulations neglect Coulomb deflection in the target and final state interaction in the three-body decay [22]. In the case of the 6.15 MeV level, the democratic and the virtual sequential decay simulations lead to similar momentum and angle correlations between the two protons, but differ from the ^2He decay, provided the correlations are studied over an angular range large enough [10]. Indeed, the relative momentum spectrum of the two protons in case of ^2He emission is characterized by an enhancement at 20 MeV/c, namely, the ^2He resonance, due to the attractive singlet s -wave interaction between the two protons [23].

The experimental spectra clearly show an enhancement at $|\vec{q}_{\text{rel}}| = 20$ MeV/c and $\theta_{\text{CM}} = 50^\circ$ as expected for the ^2He emission. The best agreement is found with $(66 \pm 9)\%$ contribution from the democratic three-body, $(3 \pm 2)\%$ from the virtual sequential and $(31 \pm 7)\%$ contribution from the ^2He decay modes.

In order to explore ^2He emission from ^{18}Ne levels, others than the 6.15 MeV, the proton-proton relative momentum spectrum for the $^{16}\text{O} + 2p$ events lying at excitation energies greater than 6.5 MeV has been analyzed (Fig. 4, left-panel). The experimental spectrum is repro-

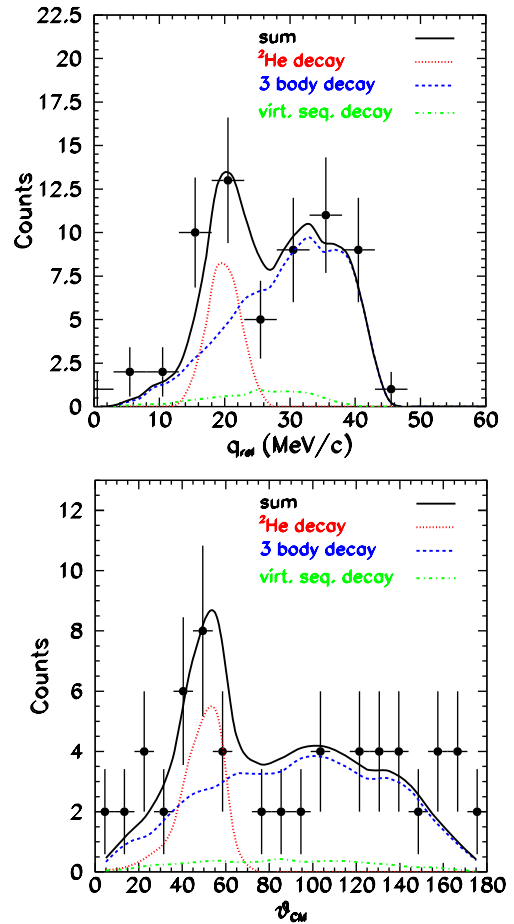


FIG. 3 (color online). Relative-momentum $|\vec{q}_{\text{rel}}|$ (top panel) and relative-angle (bottom panel) spectra, in the $^{16}\text{O} + 2p$ CM system, of the two protons emitted from the 6.15 MeV level, compared with Monte Carlo simulations.

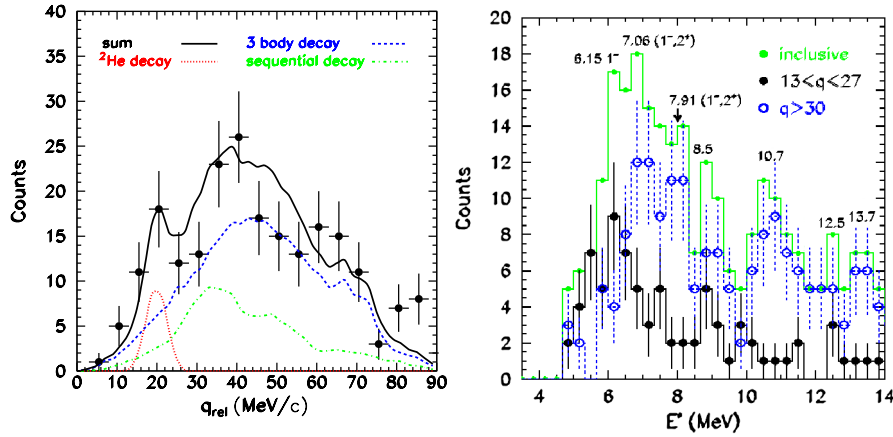


FIG. 4 (color online). Left panel: Two protons $|\vec{q}_{rel}|$ spectrum for $^{16}\text{O} + 2p$ events with $E^* > 6.5$ MeV. Right panel: Excitation-energy spectrum from inclusive $^{16}\text{O} + 2p$ events compared with those gated in the $|\vec{q}_{rel}|$ spectra of the left panel and of Fig. 3.

duced in the best way with $(64 \pm 7)\%$ contribution from the democratic, $(30 \pm 4)\%$ from the true sequential and $(6 \pm 2)\%$ contribution from the ^2He decay modes. This finding suggests the probability, although small, that high-lying levels of ^{18}Ne could decay via diproton emission. In order to disentangle the contributions of the ^{18}Ne observed levels, the excitation-energy spectrum was reconstructed both with those events lying in the relative-momentum region around 20 MeV/c ($13 < |\vec{q}_{rel}| < 27$ MeV/c) (filled symbols in Fig. 4, right panel) and with the ones lying in the relative-momentum region $|\vec{q}_{rel}| > 30$ MeV/c (open symbols in Fig. 4, right panel), where the peaks of both the democratic and true sequential decay distributions lie. The ^2He and democratic contributions to the 6.15 MeV peak are in good agreement with the results of the analysis reported in Fig. 3. The bumps at 7.06, 7.91, 10.7, and 13.7 MeV values in the spectrum gated in the $|\vec{q}_{rel}| > 30$ MeV/c region, corresponding to a flat behavior in the $13 < |\vec{q}_{rel}| < 27$ MeV/c one, clearly suggest a higher branching ratio to democratic or true sequential decay modes with respect to the ^2He one for these levels. Therefore, though the low statistics hampers quantitative conclusions, the ^2He decay contribution of $(6 \pm 2)\%$ in Fig. 4, left panel could be due to the remaining observed ^{18}Ne high-lying levels. One possible candidate could be the 8.5 MeV level as suggested in [24].

In summary, we have reported the first experimental evidence for diproton emission from the 6.15 MeV (1^-) ^{18}Ne level. The ^{18}Ne beam was produced by the ^{20}Ne projectile fragmentation on a ^9Be target at 45 AMeV. ^{18}Ne levels were populated by Coulomb excitation on a $^{\text{nat}}\text{Pb}$ target. Several levels were identified in the excitation-energy spectrum built by kinematic reconstruction from the $^{17}\text{F} + p$ and $^{16}\text{O} + 2p$ fully measured decay events. The presence of the 6.15 MeV (1^-) peak in the $^{16}\text{O} + 2p$ energy spectrum confirms the already observed two-protons decay of such level [10]. In particular, the study of the relative-momentum and angle correlation of the two protons, analyzed in the excitation-energy window $5.9 \leq E^* \leq 6.5$ MeV, clearly disentangles the diproton (31%)

and democratic or virtual sequential (69%) decay mechanisms contributions to the $2p$ emission. However, for a precise measurement of the branching ratio more statistics is needed. Moreover, in the $^{16}\text{O} + 2p$ decay channel the population of high-lying states in ^{18}Ne Coulomb excitation was observed. From the present analysis, the two-proton decay of such states seems to proceed predominantly via a democratic or true sequential decay mechanism.

*raciti@lns.infn.it

- [1] V. Goldansky, Nucl. Phys. **19**, 482 (1960).
- [2] V. Goldansky, Nucl. Phys. **27**, 648 (1961).
- [3] B. Blank and M. Ploszajczak, Rep. Prog. Phys. **71**, 046301 (2008), and reference therein.
- [4] M. J. Chromik *et al.*, Phys. Rev. C **55**, 1676 (1997).
- [5] T. Zeguerras *et al.*, Eur. Phys. J. A **20**, 389 (2004).
- [6] J. Giovinazzo *et al.*, Phys. Rev. Lett. **89**, 102501 (2002).
- [7] M. Pfützner *et al.*, Eur. Phys. J. A **14**, 279 (2002).
- [8] B. Blank *et al.*, Phys. Rev. Lett. **94**, 232501 (2005).
- [9] C. Dossat *et al.*, Phys. Rev. C **72**, 054315 (2005).
- [10] J. Gomez del Campo *et al.*, Phys. Rev. Lett. **86**, 43 (2001).
- [11] M. I. Mukha *et al.*, Nature (London) **439**, 298 (2006).
- [12] I. Mukha *et al.*, Phys. Rev. Lett. **99**, 182501 (2007).
- [13] O. V. Bochkarev *et al.*, Nucl. Phys. A **505**, 215 (1989).
- [14] L. Grigorenko, R. Johnson, I. Thompson, and M. Zhukov, Phys. Rev. C **65**, 044612 (2002).
- [15] J. Okolowicz, M. Ploszajczak, and I. Rotter, Phys. Rep. **374**, 271 (2003).
- [16] J. Rotureau, J. Okolowicz, and M. Ploszajczak, Phys. Rev. Lett. **95**, 042503 (2005).
- [17] E. Rapisarda *et al.*, Eur. Phys. J. Special Topics **150**, 269 (2007).
- [18] O. Tarasov and D. Bazin, Nucl. Phys. A **746**, 411 (2004).
- [19] G. Cardella *et al.*, AIP Conf. Proc. **961**, 105 (2007).
- [20] www.nndc.bnl.gov (2007).
- [21] J. Randrup, Comput. Phys. Commun. **59**, 439 (1990).
- [22] L. Grigorenko, R. Johnson, I. Mukha, I. Thompson, and M. Zhukov, Phys. Rev. C **64**, 054002 (2001).
- [23] S. Koonin, Phys. Lett. B **70**, 43 (1977).
- [24] Changbo Fu *et al.*, Phys. Rev. C **76**, 021603(R) (2007).